

1 **Various miRNAs are involved in efficient HCV replication**

2  
3 Chikako Ono<sup>1</sup>, Takasuke Fukuhara<sup>1\*</sup>, Songling Li<sup>2</sup>, Jian Wang<sup>3</sup>, Asuka Sato<sup>1</sup>, Takuma Izumi<sup>1</sup>, Yuzy  
4 Fauzyah<sup>1</sup>, Takuya Yamamoto<sup>1</sup>, Yuhei Morioka<sup>1</sup>, Nikolay V. Dokholyan<sup>3,4</sup>, Daron M. Standley<sup>2</sup>, and  
5 Yoshiharu Matsuura<sup>1\*</sup>

6  
7 <sup>1</sup>Department of Molecular Virology and <sup>2</sup>Department of Genome Informatics, Research Institute for  
8 Microbial Diseases, Osaka University, Osaka, Japan

9  
10 <sup>3</sup>Department of Pharmacology and <sup>4</sup>Department of Biochemistry & Molecular Biology, Penn State  
11 University College of Medicine, Hershey, Pennsylvania, United States of America

12  
13 \*Corresponding author:

14 Email; [fukut@biken.osaka-u.ac.jp](mailto:fukut@biken.osaka-u.ac.jp) (TF) or [matsuura@biken.osaka-u.ac.jp](mailto:matsuura@biken.osaka-u.ac.jp) (YM)

## 17 **Abstract**

18 One of the determinants for tissue tropism of hepatitis C virus (HCV) is miR-122, a liver-specific  
19 microRNA. Recently, it has been reported that interaction of miR-122 to HCV RNA induces a  
20 conformational change of the 5'UTR internal ribosome entry site (IRES) structure to form stem-loop II  
21 structure (SLII) and hijack of translating 80S ribosome through the binding of SLIII to 40S subunit,  
22 which leads to efficient translation. On the other hand, low levels of HCV-RNA replication have also  
23 been detected in some non-hepatic cells; however, the details of extrahepatic replication remain  
24 unknown. These observations suggest the possibility that miRNAs other than miR-122 can support  
25 efficient replication of HCV-RNA in non-hepatic cells. Here, we identified a number of such miRNAs  
26 and show that they could be divided into two groups: those that bind HCV-RNA at two locations  
27 (miR-122 binding sites I and II), in a manner similar to miR-122 (miR-122-like), and those that target a  
28 single site that bridges sites I and II and masking both G28 and C29 in the 5'UTR (non-miR-122-like).  
29 Although the enhancing activity of these non-hepatic miRNAs were lower than those of miR-122,  
30 substantial expression was detected in various normal tissues. Furthermore, structural modeling  
31 indicated that both miR-122-like and non-miR-122-like miRNAs not only can facilitate the formation of  
32 an HCV IRES SLII but also can stabilize IRES 3D structure in order to facilitate binding of SLIII to the  
33 ribosome. Together, these results suggest that HCV facilitates miR-122-independent replication in  
34 non-hepatic cells through recruitment of miRNAs other than miR-122. And our findings can provide a  
35 more detailed mechanism of miR-122-dependent enhancement of HCV-RNA translation by focusing  
36 on IRES tertiary structure.

## 37 **Author summary**

38 One of the determinants for tissue tropism of hepatitis C virus (HCV) is miR-122, a liver-specific  
39 microRNA, which is required for efficient propagation. Recently, it has been reported that interaction of  
40 miR-122 with the 5'UTR of HCV contributes to the folding of a functional IRES structure that is  
41 required for efficient translation of viral RNA. In this study, we examined the minimum motifs in the  
42 seed region of miRNAs required for the enhancement of HCV replication. As a result, we found two  
43 groups of non-hepatic miRNAs: “miR-122-like miRNAs” that can bind HCV-RNA at two locations in  
44 a manner similar to miR-122, and “non-miR-122-like miRNAs” that target a single site that masking  
45

46 both G28 and C29 in the 5'UTR. The interaction of these non-hepatic miRNAs with the 5'UTR can  
47 facilitate not only the folding of active HCV IRES but also the stabilization of IRES 3D structure in  
48 order to facilitate binding to the ribosome. These results suggest the possibility of replication of HCV in  
49 non-hepatic cells through interaction with miRNAs other than miR-122 and provide insight into the  
50 establishment of persistent infection of HCV in non-hepatic tissues that lead to the development of  
51 extrahepatic manifestations.

52

## 53 **Introduction**

54 Hepatitis C virus (HCV) infects over 71 million people worldwide and is a major cause of chronic  
55 hepatitis, liver cirrhosis and hepatocellular carcinoma [1]. One of the most important host factors for  
56 HCV infection is a liver-specific microRNA (miRNA), miR-122 [2]. On the other hand, chronic  
57 infection with HCV is often associated with extrahepatic manifestations such as mixed  
58 cryoglobulinemia, B-cell lymphoma, thyroiditis, and diabetes mellitus [3]. Supported by clinical  
59 observations, low levels of replication of HCV-RNA were detected in PBMCs and neuronal tissues in  
60 chronic hepatitis C patients [4, 5] and the treatment of chronic hepatitis C patients who developed B cell  
61 lymphoma by direct-acting antivirals for HCV resulted in the clearance of HCV and lymphoma [6].  
62 These observations suggest that the replication of HCV in non-hepatic cells can be established in  
63 miR-122-deficient condition.

64 In general, miRNAs negatively regulate translation of target mRNA through interaction with the 3'UTR  
65 in a sequence-specific manner. In this way, miR-122 regulates the expression of genes involved in the  
66 maintenance of liver homeostasis, including lipid metabolism, iron metabolism, and carcinogenesis [7,  
67 8]. In contrast, miR-122 has also been shown to stabilize HCV-RNA [9] and enhance internal ribosome  
68 entry site (IRES)-mediated translation [2, 10, 11] and replication [12] of HCV-RNA through direct  
69 interaction with the 5'UTR of HCV [13, 14]. The HCV 5'UTR has two binding sites (sites I and II),  
70 which are highly conserved among HCV genotypes [15], to which the miR-122 seed sequence can bind  
71 [2, 13]. In addition, the overhanging regions in miR-122 have been reported to interact with HCV-RNA  
72 and are important for HCV-RNA abundance [14]. Importantly, activation of translation via IRES is  
73 promoted by the Argonaut-containing miRNA-induced silencing complex (miRISC) [11]. The  
74 miR-122-miRISC complex prevents degradation of HCV-RNA by the cellular 5'-3' exonucleases Xrn1

75 and Xrn2, and stabilizes the HCV-RNA interaction [16-18]. Upon HCV infection, the interaction  
76 between miR-122-miRISC and HCV-RNA further results in the sequestration of miR-122 from host  
77 mRNA targets, a phenomenon known as the “sponge effect”, which may be responsible for the  
78 long-term oncogenic potential of HCV infection [19]. Recently, it has been reported that miR-122 has  
79 an RNA chaperone-like function that induces the folding of the HCV IRES such that in it can readily  
80 associate with the 80S ribosome for efficient translation [20, 21]. The functional HCV IRES consists of  
81 three parts: the long arm, the short arm and the body. In the liver, HCV hijacks the translating 80S  
82 ribosome by using miR-122 to alter the fold of the IRES body in order to bind to the 40S platform [22].  
83 However, it is currently unknown how persistent infection in non-hepatic cells, which are deficient in  
84 miR-122, is established.

85  
86 Previously, we and other groups have reported that an adaptive mutant possessing a G28A substitution  
87 in the 5’UTR of the HCV genotype 2a emerges during serial passages of wild type HCV in miR-122  
88 knockout cells, and that these mutants exhibit efficient RNA replication in the absence of miR-122 [23,  
89 24]. Recently, it has been reported that the G28A mutation in the 5’UTR alters the energetics of IRES  
90 folding in manner that is miR-122-independent but structurally similar to that of miR-122-mediated  
91 folding [20, 21]. Interestingly, the G28A mutation does not occur under miR-122-abundant conditions.  
92 Moreover, in clinical samples obtained from patients infected with HCV genotype 2, the rate of G28A  
93 mutation was higher in miR-122-deficient peripheral blood mononuclear cells (PBMCs) than in sera  
94 that mainly included hepatocyte-derived HCV [23]. Therefore, in this study, we examined the  
95 possibility of HCV-RNA replication in miR-122-deficient cells, such as non-hepatic cells, and of  
96 participation of miRNAs other than miR-122 to support replication of HCV-RNA.

97  
98 By mutagenesis analysis, we observed miRNA binding in a manner distinct from that of miR-122 that  
99 resulted in enhanced HCV-RNA replication. While miRNA-122 binds HCV-RNA at sites I and II  
100 using 6 matching nucleotides containing a GAGUG motif in the seed sequence, we observed a pattern  
101 wherein one miRNA molecule was bound to a position intermediate to sites I and II using 7 nucleotides.  
102 Although the ability of such miRNAs to promote HCV-RNA replication in miR-122 knockout cells  
103 was lower than that of miR-122, the expression of the miRNAs significantly enhanced viral RNA

104 replication. Furthermore, substantial expression of the miRNAs was observed in various human tissues;  
105 expression of the miRNAs enhanced HCV propagation in miR-122 knockout cells and increased viral  
106 titers by serial passages without emergence of the G28A mutation. These results suggest that HCV  
107 facilitates persistent infection in miR-122-deficient non-hepatic cells through emergence of mutant  
108 viruses and recruitment of miRNAs other than miR-122, which leads to development of extrahepatic  
109 manifestations in chronic hepatitis C patients.

110

## 111 **Results**

### 112 **Interactions between miR-122 and 5'UTR required for enhancement of HCV-RNA replication**

113 The direct interaction of two molecules of miR-122 with the 5'UTR is known to be essential for  
114 efficient HCV-RNA replication in hepatocytes (Fig 1A). One miR-122 molecule binds the HCV-RNA  
115 at positions 1-3 and 21-27 using miRNA positions 15-17 and 2-8, respectively, where the latter position,  
116 is called site I. A second miR-122 molecule binds the HCV-RNA at positions 29-32 and 37-42 using  
117 miRNA positions 13-16 and 2-7, respectively, where the latter position is called site II. To quantify the  
118 contribution of specific nucleotides in miR-122 to the enhancement of HCV-RNA replication, a library  
119 of miR-122 point-mutants was employed (Fig 1B). Variants of miR-122 possessing substitutions in the  
120 seed region and a plasmid encoding an infectious cDNA of HCV, pHH-JFH1mt, were transfected into  
121 miR-122 deficient (751-122KO) cells and intracellular HCV-RNA was determined at 3 days  
122 post-transfection. Expression of variants containing mutations at positions 1, 8 and 16 exhibited efficient  
123 enhancement of HCV-RNA replication, comparable to that of wild type miR-122 (930-fold increase)  
124 (Fig 1C). In contrast, mutation of positions 3 to 7 severely impaired HCV-RNA replication. Mutation of  
125 positions 2 and 15 resulted in 3-fold and 13.5-fold increase in HCV-RNA replication relative to control  
126 miRNA, respectively. We also examined whether the interaction of miR-122 at nucleotide positions 3-7  
127 in the seed region (GAGUG motif, red characters in Fig 1A) was sufficient to enhance HCV-RNA  
128 replication or not. The expression of a miR-122 mutant possessing the GAGUG motif with only a  
129 5-nucleotide match, miR-122-GAGUG, couldn't enhance HCV-RNA replication significantly in  
130 751-122KO cells (S1 Fig), suggesting that an miRNA possessing the GAGUG motif with a  
131 6-nucleotide match in the seed region, such as where positions 2 or 8 were mutated, would be capable of  
132 enhancing of HCV-RNA replication.

133

134 To further examine the effects of the mutations on HCV propagation, the mutant plasmids of  
135 pHH-JFH1mt were transfected into Huh7.5.1 cells and infectious titers in the culture supernatants were  
136 determined at 4 days post-transfection. HCV mutants possessing substitutions C22G, A23U, C24G,  
137 U25A, C26G, and C27G in site I, and A38U, C39G, U40A, and C41G in site II (nucleotides of HCV  
138 RNA shown in red in Fig 1A) significantly reduced infectious titers to less than 20% of wild type (Fig  
139 1D). Interestingly, HCV mutants C2G, C3G, A21U, G28C, C29G, C30G, U36A, C37G, C42G, and  
140 C43G exhibited substantial replication, consistent with the rescue of replication of HCV-RNA in  
141 751-122KO cells by the expression of miR-122 variants containing mutations at positions 1, 8, 15, or 16  
142 (Fig 1C). Nucleotides G16 and G15 in miR-122 have been shown to be required for enhanced  
143 replication of HCV-RNA by 3' overhanging to nucleotides C2 and C3 of HCV RNA, respectively [14].  
144 In addition, 5' RACE analysis revealed that a revertant virus possessing a G to C substitution has  
145 emerged after 2 rounds of passage of the C3G mutant (S2 Fig). We consistently observed a factor of 10  
146 reduction in HCV-RNA replication upon mutation G15C in miR-122 (Fig 1C), suggesting that a  
147 cytosine at position of 3 in the HCV RNA may be required for efficient propagation of HCV through  
148 interaction with miR-122. Collectively, these results suggest that nucleotide positions 22-27 in site I and  
149 38 to 41 in site II play important roles in efficient replication of HCV through interaction with miR-122.

150

151 **Fig 1. Identification of core sequence of miR-122 and 5'UTR of HCV-RNA required for the**  
152 **enhancement of viral RNA replication.** (A) Diagrams of possible interaction between HCV 5'UTR  
153 and miR-122. (B) Sequence alignment of miR-122 and its mutant derivatives, miR-122-mt1, -mt2, -mt3,  
154 -mt4, -mt5, -mt6, -mt7, -mt8, -mt15 or -mt16. (C) Intracellular HCV-RNA levels of 751-122KO cells  
155 infected with JFH1 in the presence of mimic control, miR-122 or its mutant derivatives were  
156 determined at 72 hpi by qRT-PCR. (D) Various pHH-JFH1 plasmids encoding HCV mutants at  
157 miR-122 interaction sites were transfected into Huh7.5.1 cells and infectious titers in the culture  
158 supernatants at 3 dpi were determined by focus formation assay. Error bars indicate the standard  
159 deviation of the mean and asterisks indicate significant differences (\*P < 0.05; \*\*P < 0.01) versus the  
160 results for the control.

161

## 162 **Identification of miR-122-like miRNAs that enhance HCV-RNA replication**

163 To find miRNAs other than miR-122 that could facilitate enhancement of HCV-RNA replication, we  
164 searched the miRBase database (<http://www.mirbase.org>), which contained 2656 human miRNAs, for  
165 miRNAs able to target positions 22-27 and 38-41 of HCV-RNA with a 6-nucleotide match that includes  
166 a GAGUG motif in the seed region. We identified a single miRNA (miR-504-3p) that matched all the  
167 search criteria (S3A Fig). We also identified 6 additional miRNAs (miR-574-5p, miR-3659,  
168 miR-1236-5p, miR-4481, miR-4745-5p and miR-4765) that possessed 5 complementary nucleotides in  
169 both site I and II but matched the other search criteria (S3A Fig). Among these miRNAs, we focused on  
170 3 candidates: miR-504-3p, due to its high similarity to miR-122; miR-574-5p, because it has been  
171 reported to play a functional role in neuronal cells [33, 34]; miR-1236-5p, because it has substantial  
172 expression in several tissues [34]. The tissue specificity index (TSI) can be used classify miRNAs as  
173 tissue-specific (TSI>0.85) or housekeeping (TSI<0.5) based on the expression pattern [34]. The TSI of  
174 miR-122 is 0.97, while those of miR-574-5p and miR-1236-5p are 0.79 and 0.68, respectively (S3A  
175 Fig). To confirm that the candidate miRNAs suppress translation of endogenous mRNA, a pmirGLO  
176 vector carrying the complementary sequence of each miRNA under the luciferase coding sequence was  
177 transfected into 751-122KO cells together with the corresponding miRNA mimics. Luciferase activities  
178 in 751-122KO cells transfected with the miRNA mimics of miR-122, miR-574-5p, and miR-1236-5p  
179 were strongly suppressed, while those of miR-504-3p were weakly but significantly reduced compared  
180 with those of control mimics (S3B Fig).

181  
182 Next, to examine the effect of the candidate miRNAs on the enhancement of HCV-RNA replication,  
183 751-122KO cells transfected with each miRNA mimic were infected with HCV 12 hours  
184 post-transfection and intracellular HCV-RNA was determined at 72 hours post-infection. Exogenous  
185 expression of miR-504-3p, miR-574-5p and miR-1236-5p enhanced HCV-RNA replication 50-, 20-  
186 and 5-fold, respectively, while that of mutants possessing a single mutation in the GAGUG motif,  
187 miR-504-3p-mt6, miR-574-5p-mt5 and miR-1236-5p-mt5 (Fig 2B), exhibited no enhancement (Fig  
188 2C). Compared with miR-122, the candidate miRNAs have a mismatch sequence at nucleotide  
189 positions 8 or 1 in the interacting region with HCV-RNA (Fig 2B). Interestingly, mutant miRNAs  
190 containing a modified seed sequence to complement that of HCV-RNA, exhibited significant

191 enhancement of HCV-RNA replication; in particular, the miR-574-5p mutant showed enhancement  
192 comparable with miR-122 (Fig 2D). These results imply that the candidate miRNAs participate in the  
193 enhancement of HCV-RNA replication via their GAGUG-containing region.

194

195 **Fig 2. miR-504-3p, miR-574-5p and miR-1236-5p can enhance HCV-RNA replication via**

196 **miR-122-type interaction.** (A) Diagrams of possible interaction between HCV 5'UTR and

197 miR-504-3p, miR-574-5p and miR-1236-5p. (B) Sequence alignment of miR-122, miR-504-3p,

198 miR-504-3p-mt6, miR-504-3p-mt8, miR-574-5p miR-574-5p-mt5, miR-574-5p-addG, miR-1236-5p,

199 miR-1236-5p-mt5 and miR-1236-5p-addG. Mismatching nucleotides were shown in red. (C, D)

200 Intracellular HCV-RNA levels of 751-122KO cells infected with JFH1 in the presence of mimic control,

201 miR-122, miR-504-3p, miR-574-5p and miR-1236-5p or their mutant derivatives were determined at

202 72 hpi by qRT-PCR. The data are representative of three independent experiments. Error bars indicate

203 the standard deviation of the mean and asterisks indicate significant differences (\*\* $P < 0.01$ ) versus the

204 results for the control.

205

206 **Engineered non-miR-122-like miRNAs binding to a single site in the 5'UTR are able to enhance**

207 **HCV-RNA replication.**

208 Recently, Schult and colleagues have shown that the interaction of miR-122 with the 5'UTR of HCV  
209 alters the structure of the IRES, resulting in the folding of a functional form to promote translation [20].

210 Based on this report and our observation that candidate miRNAs possessing only a 6-nucleotide match

211 also enhanced the replication of HCV, we hypothesized that modes of targeting HCV 5'UTR positions

212 23-40 other than that used by miR-122 might exist. Specifically, we examined the possibility of a single

213 miRNA binding site that bridged sites I and II. To test this hypothesis, we prepared mimic miRNAs

214 where a single complimentary site in HCV-RNA would be targeted by 6, 7 or 8 complimentary

215 nucleotides in the miRNA (S4A Fig). 751-122KO cells transfected with each mimic miRNA were

216 infected with HCV and intracellular HCV-RNA was determined at 72 hours post-infection. Among the

217 6-nucleotide matching mimics we examined, four exhibited slight enhancement of HCV-RNA

218 replication (S4B Fig). In addition, four of the mimics possessing a 7-nucleotide match to HCV-RNA

219 (Fig 3A) enhanced viral replication upon infection with HCV (Fig 3B). Interestingly, not only the



220 mimic possessing a 7-nucleotide match targeting positions 30-36 but also 8-nucleotide match targeting  
221 positions 29-36 (Fig 3A) exhibited no effect on HCV-RNA replication upon infection with HCV (Fig  
222 3B). These results suggest that miRNAs binding to a single site masking both G28 and C29 in the  
223 5'UTR with a 7-nucleotide match are able to enhance HCV-RNA replication. We denote this binding  
224 mode as “non-miR-122 like”.

225

### 226 **Natural non-miR-122-like miRNAs enhance HCV-RNA replication.**

227 To find natural non-miR-122-like miRNAs, we screened human miRNAs masking G28 and C29  
228 between stem loop I and II of HCV RNA with at least a 7-nucleotide match in the seed region. In this  
229 way, two non-miR-122-like candidates (miR-25-5p and miR-4730), with 7 and an 8-nucleotide  
230 matches, respectively, were identified (Fig 3C and S3A Fig). In addition, we used miR-652-3p, with a  
231 6-nucleotide match, as a negative control (Fig 3C and S3A Fig). To confirm the activities of each  
232 miRNA to suppress translation of target genes, pmirGLO vectors carrying the complementary sequence  
233 of each miRNA under the luciferase sequence were transfected into 751-122KO cells. Suppression of  
234 luciferase activity was observed in 751-122KO cells transfected with each of miRNA mimics compared  
235 to control mimic (S3B Fig). Next, to determine the effect of these miRNAs on HCV-RNA replication,  
236 751-122KO cells transfected with each of the miRNA mimics were infected with HCV and intracellular  
237 viral RNA was determined at 72 hours post-infection. Transduction of miR-25-5p and miR-4730  
238 exhibited approximately 60-fold enhancement of HCV-RNA replication, in contrast to that of  
239 miR-652-3p, which showed no effect on viral replication (Fig 3D). These results suggest that  
240 non-miR-122-like miRNAs binding to single site on HCV-RNA between stem loop I and II via a 7- or  
241 8-nucleotide match have the ability to enhance HCV-RNA replication.

242

### 243 **Fig 3. miR-25-5p and miR-4730 can enhance HCV-RNA replication via non-miR-122-type**

244 **interaction.** (A) Diagrams of possible interaction between HCV 5'UTR and synthetic miRNAs with  
245 7nt-match and 8nt-match. Gray-shaded area and framed by dashed line in gray indicate possible  
246 interaction region and G-U wobble pair, respectively. Nucleotides in red are important region for the  
247 enhancement by miR-122 shown in Fig 1D. (B) Sequence alignment of miR-122 and synthetic  
248 miRNAs with 7nt-match and 8nt-match. Mismatching nucleotides were shown in red. (C) Intracellular

249 HCV-RNA levels of 751-122KO cells infected with JFH1 in the presence of mimic control, miR-122,  
250 miR-122-mt6 and synthetic miRNAs with 7nt-match shown in Fig 3A. (D) Intracellular HCV-RNA  
251 levels of 751-122KO cells infected with JFH1 in the presence of mimic control, miR-122, miR-122-mt6,  
252 miR-25-5p, miR-652-5p, miR-1236-5p and miR-4730 were determined at 72 hpi by qRT-PCR. The  
253 data are representative of three independent experiments. Error bars indicate the standard deviation of  
254 the mean and asterisks indicate significant differences (\*\*P < 0.01) versus the results for the control.

255

### 256 **Expression of miR-122-like and non-miR-122-like miRNAs enhance translation of HCV RNA.**

257 Next, to determine the effect of the miRNAs on the translation of HCV RNA,  
258 SGR-GND-JFH1-NlucSec RNA, a subgenomic HCV RNA possessing Nanoluc luciferase (NlucSec)  
259 gene and a polymerase-dead mutation (S5A Fig), was electroporated into 751-122KO cells together  
260 with miRNA mimics. NlucSec activity in 751-122KO cells transduced with mimics of miR-122,  
261 miR-122-like (miR-504-3p, miR-1236-5p, miR-574-5p) and non-miR-122-like (miR-25-5p), was  
262 higher (in this order), than that of a control mimic (S5B Fig). These results suggest that these miRNAs  
263 can facilitate efficient translation of HCV genome.

264

### 265 **Expression of miRNAs other than miR-122 exhibit marginal enhancement on the replication of** 266 **genotype 1b HCV.**

267 Because sequences between stem loop I and II of HCV are different among HCV genotypes and  
268 genotype 1b has G28A, G33A and A34G in the stem loop region, we examined the sequence  
269 specificity of the enhancement of HCV-RNA replication by miRNAs. miR-6880-5p was identified as a  
270 genotype 1b specific non-miR-122 type miRNA (S6A Fig). To examine the enhancement of replication  
271 of genotype 1b HCV by miRNAs, 751-122KO cells transfected with mimics of miRNAs (S6A and  
272 S6B Figs) were infected with chimeric HCV of genotype 1b Con1 strain and genotype 2a JFH1 strain  
273 (Con1C3/JFH) [23]. Among the miRNAs we examined, transfection of mimics of miR-504-3p and  
274 miR-574-5p exhibited slight but significant enhancement of replication of the chimeric HCV compared  
275 to control mimics, in contrast to large enhancement by that of miR-122 (S6C Fig). These results suggest  
276 that expression of miRNAs other than miR-122 exhibit marginal enhancement on the replication of  
277 genotype 1b HCV.

278

279 **Identification of miRNAs that suppress emergence of the G28A mutant of HCV in**  
280 **miR-122-deficient conditions.**

281 To examine the emergence of the G28A mutation of HCV during serial passages in the presence of  
282 candidate miRNAs, 751-122KO cells transfected with either miRNA mimics of miR-122,  
283 miR-122-like (miR-504-3p, miR-574-5p, miR-1236-5p) or non-miR-122-like (miR-25-5p) were  
284 infected with HCV and infectious titers in the culture supernatants were determined at each passage (Fig  
285 4A). At passages 3 and 6, we determined the sequence of the 5'UTR of HCV by direct sequencing. The  
286 G28A mutation emerged by 6 passages of HCV in 751-122KO cells expressing either control or  
287 miR-574-5p mimic, but not in those of other miRNAs (Fig 4B). In addition, expression of miR-122 and  
288 miR-574-5p enhanced replication of the G28A mutant of HCV approximately 30- and 4-fold,  
289 respectively, probably due to higher affinity than wild type HCV, but that of miR-25-5p, miR-504-3p  
290 and miR-1236-5p exhibited no enhancing effect (S7A and S7B Figs). These results suggest that  
291 presence of miR-122, miR-25-5p, miR-504-3p and miR-1236-5p suppresses the emergence of the  
292 G28A mutation in HCV and that HCV facilitates replication in miR-122-deficient conditions through  
293 not only emergence of mutants but also recruitment of miRNAs other than miR-122.

294

295 **Fig 4. The effect of miRNAs on HCV propagation and the introduction of G28A mutation. (A)**  
296 Infectious titer in the culture medium on serial passage of 751-122KO cells in the presence of mimic  
297 control, miR-122, miR-25-5p, miR-504-3p, miR-574-5p and miR-1236-5p. (B) Mutation of G28A in  
298 the 5'UTR of HCV was identified in all independently isolated HCV propagated in Fig 4A. Arrows  
299 indicate the position of nt28 in the 5'UTR of HCV. Each RNA base is represented as a colored peak: A,  
300 green; U, red; G, black; and C, blue.

301

302 **3D modeling of the miRNA: HCV-RNA:Ago2 complex.**

303 In this study, we have shown that not only miR-122-like miRNAs but also non-miR-122-like miRNAs  
304 can enhance HCV-RNA translation (S5B Fig) and replication. (Fig 3D). Recent studies have revealed  
305 that binding of an miR-122:Ago2 complex or introduction of nucleotide substitutions, such as the G28A  
306 mutation, facilitate efficient translation by making an HCV IRES stem-loop (SLII, "long arm")

energetically favorable [20, 21]. More recently, HCV IRES has been reported to hijack the translating 80S ribosome by interaction between the HCV IRES body to the 40S subunit [22]. We hypothesized that the binding of one non-miR-122-like miRNA with a 7-nucleotide match (miR-25-5p) can similarly alter the IRES structure. In contrast, binding of a negative control (miR-652-3p), with only a 6 nucleotide match, is predicted not to alter the IRES structure favorably (Fig 3D). In order to test these hypotheses, we docked representative miRNAs to HCV-RNA, and carried out Replica-Exchange Molecular Dynamics, which can thoroughly sample the resulting conformational space. Specifically, we examined whether miRNA binding would affect the stability of the HCV RNA body or short arm, which are expected to affect HCV RNA binding to the ribosome. 5 representative HCV IRES-miRNA complex models of each representative miRNA molecule were superimposed onto a Cryo-EM reference structure of the HCV IRES bound to the human ribosome, Protein Data Bank (PDB) entry 5a2q, via long arm SLII 39-117 (Fig 5A, top), and the spatial distribution of the body and short arm region were checked by computing the root-mean-square deviation (RMSD) among the models. As shown in Fig 5B, the RMSD of the HCV IRES body and short arm from miR-122 and miR-25-5p were significantly smaller than that of miR-652-3p. Statistical analysis indicated that miR-122 and miR-25-5p were significantly similar, while miR-652-3p was significantly different. This, in turn, suggests that the HCV IRES body and short arm of the miR-652-3p-bound RNA are structurally unstable. In spite of the fact that miR-122 and miR-25-5p interact with HCV-RNA differently, the effect on the stability of the HCV IRES is comparable and distinct from the negative control (miR-652-3p), which interacts with only a 6-nucleotide match. These results indicate that the conformational stability of IRES structure is important for the translational activity of HCV IRES.

**Fig 5. Model of miRNA:HCV-RNA interaction.** (A) Superposition results of HCV-RNA tertiary structure onto a Cryo-EM reference structure of the HCV IRES bound to the human ribosome. Representative models of each miRNA (top) were displayed. miRNA binding regions and long arm composed of SLII (nt1-117: blue) and SLIIIIa-IIIId (nt118-333: red) of HCV-RNA, miRNAs (blue) and 40S rRNA subunit (gray) were shown. Representative models of each miRNA:HCV-RNA:Ago2 (bottom). The distribution of tertiary structures of SLIIIIa-IIIId were shown as gray sphere. (B) Box-plots of pairwise RMSDs among models of HCV region (SLIIIIa-IIIId: nt118-333, red blocks in Fig 5A, top).

336 All pairwise RMSDs among 5 representative models (Fig 5A) of nt118-333 regions were determined.  
337 The bottom and top boundaries of the box correspond to Q1 (25<sup>th</sup> percentile) and Q3 (75<sup>th</sup> Percentile)  
338 quartiles, respectively. The lower and upper whiskers correspond to  $Q1 - 1.5 * IQR$  and  $Q3 + 1.5 * IQR$ ,  
339 respectively, where  $IQR = Q3 - Q1$ . Median value (Q2, 50<sup>th</sup> percentile) is indicated by an orange line  
340 within the box, and mean value is indicated by a triangle symbol in green. Asterisks indicate significant  
341 differences (\*\*P < 0.01, n.s.: not significant).

342  
343 Next, to infer the binding mode of Ago2 on the HCV IRES-miRNA complex model, a complex model  
344 was built using PDB entry 6n4o. Specifically, the Ago2 structure was incorporated into the  
345 HCV-miRNA models superimposing the double stranded RNA region at the 5' end of miR-122 and  
346 complimentary strand in the HCV-RNA. S8 Fig show alternative binding conformations of Ago2 on  
347 different representative HCV-miRNA models. We found that most molecular dynamics snapshots  
348 could accommodate Ago2 binding, which is consistent with the previous reports that the formation of  
349 SLII of functional IRES is mediated by the interaction with Ago2-miRNA.

350

### 351 **miRNAs other than miR-122 may facilitate HCV-RNA replication in various tissues.**

352 Finally, to examine the possibility of participation of miRNAs other than miR-122 in the replication of  
353 HCV in non-hepatic cells, expression of the candidate miRNAs in normal tissues was determined by  
354 qRT-PCR. Although expression of miR-25-5p, miR-504-3p, miR-574-5p and miR-1236-5p were  
355 significantly lower than that of miR-122 in liver, these miRNAs were detected in various normal tissues  
356 including brain, thyroid, lung, stomach, small intestine, colon, kidney, liver and bone marrow (S9 Fig).  
357 Interestingly, miR-504-3p is expressed mainly in non-hepatic tissues. These observations suggest that  
358 not only liver-specific miR-122 but also other miRNAs, such as miR-25-5p, miR-504-3p, miR-574-5p  
359 and miR-1236-5p, expressed in various tissues, can facilitate HCV-RNA replication in non-hepatic  
360 tissues.

361

## 362 **Discussion**

363 In this study, we examined the possibility of involvement of miRNAs other than liver-specific miR-122  
364 in the enhancement of HCV-RNA replication and showed that HCV-RNA replication is enhanced by

365 the binding of non-hepatic miRNAs. We found that HCV-RNA can be targeted by miR-122-like  
366 miRNAs with 6 matching nucleotides containing a GAGUG motif at two sites (sites I and II). Such  
367 miRNAs include miR-504-3p, miR-574-5p, miR-1236-5p. In addition, HCV-RNA can also be targeted  
368 by non-miR-122-like miRNAs with at least 7 matching nucleotides that can mask G28 and C29 and  
369 bind a single site between sites I and II. Such miRNAs include miR-25-5p and miR-4730. Recently, it  
370 has been reported that the interaction of miR-122 with the 5'UTR of HCV alters the structure of the  
371 IRES, resulting in folding of a functional form to promote translation [20]. Based on the secondary  
372 structure of HCV-RNA predicted by selective 2'-hydroxyl acylation analyzed by primer extension  
373 (SHAPE), a stem including positions 21-29 was shown to be the minimum free energy structure [20,  
374 35]. In addition, another stem structure including positions 27-33 was predicted as the lowest free  
375 energy structure by *in silico* RNA structure prediction algorithms [21]. Although both structures lack  
376 stem-loop II (SLII) and fail to form a functional HCV IRES, only a single (G28A) substitution in the  
377 5'UTR of the HCV genotype 2a has been implicated in the folding of SLII without miR-122 binding  
378 [20]. These observations suggest that the interruption of base pair of G28 and C29 promotes translation  
379 through the formation of SLII. Therefore, it is reasonable to hypothesize that the binding of miRNAs to  
380 HCV RNA perturbs the minimum free energy structure, leading to efficient formation of SLII, which,  
381 in turn, can be facilitated by the disruption of stem structures including G28 and C29 in the 5'UTR.

382  
383 Although non-miR-122-like miR-652-3p can interact with the HCV 5'UTR via G28 and C29, which  
384 promotes the formation of the SLII structure based on 2D predictions, it did not enhance HCV RNA  
385 replication (Fig 3D). We therefore focused on the 3D structural dynamics of the  
386 HCV-RNA:miRNA:Ago2 complex. Our 3D structural modeling suggested the importance of  
387 conformational stability of the IRES body structure for efficient translation (Fig 5A and 5B). The  
388 identification of the HCV IRES tertiary structure by Cryo-EM revealed that it consists of three parts: a  
389 long arm (SLII), a body and a short arm [22]. The interaction of the body with the 40S subunit and the  
390 structure of the long arm are important for the initiation of translation of HCV IRES [22]. It has been  
391 shown that HCV IRES captures the actively translating 80S ribosome and remains bound to the 40S  
392 subunit via interactions with the body after translation termination of the 5'-capped mRNA; HCV IRES  
393 subsequently places its downstream RNA onto the 40S subunit using the long arm [22]. Based on these

394 observations and our modeling results, it appears that not only the formation of SLII in the HCV 5'UTR,  
395 but also alteration of structural dynamics, especially the conformational stability of body, as mediated  
396 by the binding of miRNA with Ago2, is required for functional IRES formation. Further studies are  
397 needed to clarify the stabilizing effects of non-miR-12-like miRNAs on the HCV IRES structure.

398

399 We also observed that, in the presence of either miR-122-like or non-miR-122-like miRNAs, the  
400 emergence of the G28A mutation in HCV was suppressed (Fig 4). Our previous report showed that  
401 wild type G28 virus was still detected in miR-122-deficient PBMCs from patients infected with  
402 genotype 2a HCV and that the G28A mutant exhibited lower replication than wild type in the presence  
403 of miR-122 [23]. These observations suggest that the G28A mutant interacting with an Ago2-miRNA  
404 complex, mediated by not only miR-122 but also non-hepatic miRNAs, has disadvantages in stages of  
405 the viral life cycle other than translation, such as replication, assembly or particle production in  
406 miRNA-abundant conditions. Although the involvement of miRNAs in viral particle formation has not  
407 been well-studied, it has been reported that the binding of miRNAs such as miR-155 and miR-92a to  
408 the HIV-1 genomic RNA can increase efficiency of the packaging of the miRNAs into virions [36].  
409 Because a high level of miRNA incorporation significantly inhibited HIV-1 replication and virion  
410 infectivity, it was hypothesized that RNA viruses such as HIV-1 have evolved to avoid cellular miRNA  
411 binding to their genome [36]. Other groups have also reported that the regulation of HIV latency by  
412 several miRNAs in CD4<sup>+</sup>T cells and their inhibition resulted in the enhancement of viral protein  
413 expression and particle production [37]. On the other hand, a cis-acting element for HCV-RNA  
414 packaging process has been identified as the 3'X region consisting of stem-loop I, II and III in 3'UTR  
415 [38] but not in the 5'UTR [39]. Moreover, G28A mutant can easily form SLII in miRNA-independent  
416 manner, which is advantageous for translation step, in contrast, it might be not suitable for the  
417 replication or particle formation step in the presence of miR-122. Further studies are needed to  
418 determine the role of the interaction of miRNA with HCV RNA and the advantages of guanine at 28 in  
419 genotype 2a HCV in miR-122-abundant conditions, especially focusing on post-translation step of  
420 HCV life cycle.

421

422 From an evolutionary perspective, among seven genotypes of HCV, gt2 is predicted to be the oldest  
423 lineage, followed by genotypes of 3, 5, and 6 [40]. On the other hand, genotypes of 1 and 4 emerged  
424 more recently. Furthermore, characteristic distribution of HCV genotypes different geographical regions  
425 [41]. Accordingly, sequences around the miR-122 interaction sites are different among genotypes of  
426 HCV [13], for example, the nucleotide position 28 of HCV genome is guanine and adenine in genotype  
427 2 and genotypes of 1, 3, and 4, respectively. These differences of 5'UTR sequence may affect the  
428 dependence on miRNAs for translation. Supporting that, we observed the replication of chimeric HCV  
429 of genotypes 1 and 2, Con1/JFH, was also enhanced by miRNAs other than miR-122 in genotype 2a  
430 JFH-1 strain, while the enhancing effect on replication of Con1/JFH by miR-122-like miRNAs was  
431 significantly lower than that by miR-122 (Fig 2C and S6C Fig). In addition, although mutagenesis  
432 analysis of the miR-122 binding site in genotype 1a H77 strain has shown that the overhanging  
433 nucleotide positions of 15 and 16 in miR-122 are required for efficient replication of HCV [14], in this  
434 study, we demonstrated that interaction with nucleotide positions 15 or 16 in miR-122 are dispensable  
435 for the enhancement of replication of genotype 2a JFH-1 strain (Fig 1C). These observations suggest  
436 that the dependence on miRNAs for the enhancement of HCV-RNA replication is different among  
437 genotypes, which may be a survival strategy acquired during HCV evolution.

438  
439 Furthermore, enhancement of HCV-RNA replication by miRNAs other than miR-122 might be  
440 involved in the genotype-specific propagation and pathogenesis by the “sponge effect” [19], which is  
441 caused by the sequestration of miRNAs by the replication of viral genome, leading to the de-repression  
442 of the host target mRNAs. Amyloid precursor protein regulates neurogenesis by antagonizing  
443 miR-574-5p in the developing cerebral cortex which promotes neurogenesis [33]. miR-574-5p also  
444 participates in the promotion of metastasis and invasion of lung cancer through PTPRU (protein tyrosine  
445 phosphatase, receptor type U) [42, 43] and TLR9 signaling [44]. In addition, miR-25-5p has been shown to  
446 inhibit cell proliferation of colorectal cancer through activation of AMP-activated protein kinase  
447 (AMPK) signaling by silencing protein kinase C  $\zeta$  [45], suggesting that sequestering of miR-25-5p  
448 activates cancer cell proliferation and affects regulation of energy metabolism and maintenance of  
449 glucose homeostasis mediated by AMPK signaling [46]. Further studies are needed to clarify the roles



450 of sequestration of miRNAs such as miR-574-5p and miR-25-5p by the replication of HCV in the  
451 development of extrahepatic manifestations.

452

453 In this study, we have shown the possibility of replication of HCV through interaction with miRNAs  
454 other than miR-122 in non-hepatic cells, which is required for the conformational change and  
455 stabilization of IRES tertiary structure. These observations provide those miRNAs may lead to the  
456 development of extrahepatic manifestations in chronic hepatitis patients through persistent infection of  
457 HCV. And we also demonstrate the importance of the 3D structure prediction of IRES through the  
458 simulation of HCV RNA:miRNA:Ago2 complex. This technique can be a powerful tool for design of  
459 novel anti-HCV drug or treatment targeting HCV-specific system to hijack host translational  
460 machinery.

461

## 462 **Materials and Methods**

463 **Plasmids.** pCSII-EF-WT-miR-122 and pCSII-EF-AcGFP were described previously [23], respectively.  
464 Various mutants of pHH-JFH1mt (pHH-JFH1-E2p7NS2mt; described in [23]) were established by the  
465 introduction of a point mutation in miR-122 binding sites of 5'UTR. The complementary sequences of  
466 miR-122-5p miR-25-5p, miR-504-3p, miR-574-5p, miR-1236-5p, miR-652-5p, miR-4730 and  
467 miR-8074 were introduced into the multicloning site of the pmirGLO vector (Promega, Tokyo, Japan).  
468 The plasmid pX330 (Addgene plasmid 42230) designed for the CRISPR-Cas9 system [25, 26] was  
469 provided by Addgene. pSGR-GND-JFH1 was established by the introduction of a point mutation of  
470 D2760N (from GDD to GND) located in the NS5B polymerase coding region of the pSGR-JFH1. The  
471 secreted Nanoluc (Nlucsec) fragment from the pNL1.3 vector (Promega, Madison, WI) was replaced  
472 with the neomycin gene of pSGR-GND-JFH1 and the resulting plasmid was designated  
473 pSGR-GND-JFH1-Nlucsec. The plasmids used in this study were confirmed by sequencing with an  
474 ABI PRISM 3130 genetic analyzer (Life Technologies, Tokyo, Japan).

475

476 **Cells, mimic miRNAs and transfection.** Human hepatocellular carcinoma cell line Huh7, human  
477 embryonic kidney cell line 293T was obtained from Japanese Collection of Research Bioresources Cell  
478 Bank (JCRB0403 and JCRB9068). The Huh7-derived hepatocellular carcinoma cell line Huh7.5.1 cells

479 were provided by F. Chisari. All cell lines were maintained in Dulbecco's modified Eagle's medium  
480 (DMEM) (Sigma, St. Louis, MO) supplemented with 100 U/ml penicillin, 100 µg/ml streptomycin and  
481 10% fetal bovine serum (FBS), and cultured at 37°C under the conditions of a humidified atmosphere  
482 and 5% CO<sub>2</sub>. Cells were transfected with the plasmids by using *Trans* IT LT-1 transfection reagent  
483 (Mirus, Madison, WI) according to the manufacturer's protocols. All mimic miRNAs were obtained  
484 from Gene Design (Osaka, Japan) and transfected into cells using Lipofectamine RNAi MAX (Life  
485 Technologies) according to the manufacturer's protocol.

486

487 **Viruses.** pHH-JFH1-E2p7NS2mt was transfected into Huh7.5.1 cells, and the culture supernatants were  
488 collected after serial passages. Infectivity of HCV was determined by focus-forming assay and  
489 expressed in focus-forming units (FFU) [27]. Unless otherwise noted, cells were infected with HCV at a  
490 multiplicity of infection of 1. The lentiviral vectors and ViraPower Lentiviral Packaging Mix (Life  
491 Technologies, San Diego, CA) were co-transfected into 293T cells and the supernatants recovered at 48  
492 h post-transfection were centrifuged at 1000 x g for 5 min and cleared through a 0.45 µm filter. The  
493 infectious titer of lentivirus was determined by a Lenti-X™ qRT-PCR Titration Kit (Clontech,  
494 Mountain View, CA).

495

496 **Total RNAs from normal tissues and quantitative RT-PCR.** Total RNAs from normal tissues such  
497 as brain, thyroid, lung, stomach, small intestine, colon, kidney, liver and bone marrow were obtained  
498 from Biochain (Newark, CA) and those from cell lines were prepared by using an PureLink® RNA mini  
499 kit (Thermo Scientific). Quantitative RT-PCR was performed by using TaqMan® RNA-to-Ct™ 1-Step  
500 Kit and a ViiA7 system (Thermo Scientific) according to the manufacturer's protocol. For quantitation  
501 of miRNA, total RNA was prepared from cells by using an miRNeasy mini kit (Qiagen) and mature  
502 miR-122-5p, miR-504-3p or miR-574-5p were reverse transcribed by using TaqMan™ Advanced  
503 miRNA cDNA Synthesis Kit (Thermo Scientific) and then amplified by using specific primers  
504 provided in the TaqMan Advanced miRNA Assays (Thermo Scientific) according to the  
505 manufacturer's protocol. miR-25-3p was used as an internal control [28]. Fluorescent signals were  
506 analyzed by using a ViiA7 system.

507

508 **Analysis of the 5'UTR sequence of HCV.** For a rapid identification of 5'UTR sequence of HCV,  
509 RNAs extracted from 100 µl of virus-containing supernatants or PBMCs were amplified by using a  
510 PrimeScript® RT reagent Kit (Perfect Real Time) (Takara Bio) and 5'RACE was performed by using a  
511 5'RACE System for Rapid Amplification of cDNA Ends, Version 2.0 (Life Technologies) as described  
512 by Ono et al. [23].

513

514 ***In vitro* transcription and RNA electroporation.** The plasmids pSGR-GND-JFH1-Nlucsec and  
515 pJFH1-E2p7NS2mt were linearized by XbaI and transcribed *in vitro* by using the MEGAscript T7 kit  
516 (Life Technologies) according to the manufacturer's protocol. Capped and polyadenylated firefly  
517 luciferase (Fluc) RNAs were synthesized by using a mMACHINE T7 Ultra kit (Life  
518 Technologies) according to the manufacturer's protocol. The *in vitro* transcribed RNA from  
519 pSGR-JFH1 (5 µg) was electroporated into cells at 5x10<sup>6</sup> cells/0.4 ml under conditions of 220V and  
520 950 µF using a Gene Pulser™ (Bio-Rad, Hercules, CA) and plated on DMEM containing 10% FBS.

521

522 **Analysis of HCV IRES translation activity.** *In vitro* transcribed JFH1-NlucSec GND-SGR RNA (5  
523 µg) was electroporated together with Fluc RNA (2 µg) as described above and plated on DMEM  
524 containing 10% FBS. Each 3 h post-electroporation, the culture media were harvested and Nanoluc  
525 activity was determined in 10 µl aliquots of culture medium using a Nano-Glo™ Luciferase Assay  
526 System (Promega). To normalize the electroporation efficiency, each cell was lysed in 50 µl of reporter  
527 lysis buffer (Promega) at 9 h post-electroporation and luciferase activity was measured in 10 µl aliquots  
528 of the cell lysates using a Luciferase Reporter Assay System (Promega).

529

530 **Luciferase assay.** Cells seeded onto 48-well plates at the concentration of 3 x 10<sup>4</sup> cells/well were  
531 transfected with 250 ng of each of the pmirGLO plasmids and were stimulated with the appropriate  
532 ligands for 24 h at 24 h post-transfection. Cells were lysed in 100 µl of passive lysis buffer (Promega)  
533 and luciferase activity was measured in 3 µl aliquots of the cell lysates using a Dual-Luciferase Reporter  
534 Assay System (Promega). Firefly luciferase activity was normalized with that of Renilla luciferase.

535

536 **Docking simulation and modeling.** First, we established the secondary structures of HCV-RNA  
537 (residues 1-289), miRNA-122 (Fig 1), miR-504-3p (Fig 2), miR-1236-5p, miR-574-5p, miR-25-5p (Fig  
538 3), miR-4730 and miR-652-3p, respectively. In order to predict the intact structures of HCV-miRNA  
539 complex, we utilize the cryo-EM structure of HCV (PDB ID: 5A2Q) as restraints to perform iFoldRNA  
540 simulation [29, 30]. iFoldRNA is an automatic and accurate RNA 3D structure prediction tool, which is  
541 developed on the basis of discrete dynamics simulation (DMD) [31, 32]. Distances between C1' atoms  
542 in 5A2Q are extracted from its 3D structure as restraints to facilitate the RNA modeling by iFoldRNA.  
543 iFoldRNA first builds a ring structure composed of all residues in the complex. Then, it conducts a  
544 10000-step initial molecular dynamics simulation to build a preliminary structure. Next, iFoldRNA  
545 utilizes replica exchange molecular dynamics simulation (REMD) to thoroughly search through the  
546 conformation space. The temperatures of the 8 threads dispatched in REMD are distributed from 0.2 to  
547 0.4 kT. Subsequently, the structures extracted from all 8 trajectories generated by REMD are ranked  
548 based on their respective free energies, and the 1% lowest free energy structures are clustered with a  
549 specific RMSD cutoff, which is typically one-tenth the number of residues. Since iFoldRNA utilizes a  
550 coarse-grained model to expedite the simulation process, the centroids of these clusters will be subject to  
551 all-atom reconstruction processes to generate the final all-atom candidate structures of the  
552 HCV-miRNA complex.

553

554 **Statistical analysis.** The data for statistical analyses are the average of three independent experiments.  
555 Results were expressed as the means  $\pm$  standard deviation. The significance of differences in the means  
556 was determined by Student's *t*-test.

557

## 558 **Acknowledgements**

559 We thank M. Tomiyama for her secretarial work, M. Ishibashi, K. Takeda for their technical assistance  
560 and M. Hijikata, T. Wakita, R. Bartenschlager, F. Chisari, and M. Whitt for providing experimental  
561 materials.

562

563

564

## References

- 565
- 566 1. WHO | Global hepatitis report, 2017. WHO. 2017. doi:
- 567 [/entity/hepatitis/publications/global-hepatitis-report2017/en/index.html](#).
- 568 2. Jopling CL, Yi M, Lancaster AM, Lemon SM, Sarnow P. Modulation of hepatitis C virus
- 569 RNA abundance by a liver-specific MicroRNA. *Science*. 2005;309(5740):1577-81. doi:
- 570 [10.1126/science.1113329](#). PubMed PMID: 16141076.
- 571 3. Galossi A, Guarisco R, Bellis L, Puoti C. Extrahepatic manifestations of chronic HCV
- 572 infection. *J Gastrointest Liver Dis*. 2007;16(1):65-73. PubMed PMID: 17410291.
- 573 4. Castillo I, Rodríguez-Iñigo E, Bartolomé J, de Lucas S, Ortiz-Movilla N, López-Alcorocho
- 574 JM, et al. Hepatitis C virus replicates in peripheral blood mononuclear cells of patients with occult
- 575 hepatitis C virus infection. *Gut*. 2005;54(5):682-5. doi: [10.1136/gut.2004.057281](#). PubMed PMID:
- 576 [15831916](#); PubMed Central PMCID: [PMCPMC1774478](#).
- 577 5. Wilkinson J, Radkowski M, Laskus T. Hepatitis C virus neuroinvasion: identification of
- 578 infected cells. *J Virol*. 2009;83(3):1312-9. doi: [10.1128/JVI.01890-08](#). PubMed PMID: 19019968;
- 579 PubMed Central PMCID: [PMCPMC2620915](#).
- 580 6. Maciocia N, O'Brien A, Ardeshta K. Remission of Follicular Lymphoma after Treatment
- 581 for Hepatitis C Virus Infection. *N Engl J Med*. 2016;375(17):1699-701. doi: [10.1056/NEJMc1513288](#).
- 582 PubMed PMID: [27783921](#).
- 583 7. Hsu SH, Wang B, Kota J, Yu J, Costinean S, Kutay H, et al. Essential metabolic,
- 584 anti-inflammatory, and anti-tumorigenic functions of miR-122 in liver. *J Clin Invest*.
- 585 2012;122(8):2871-83. doi: [10.1172/JCI63539](#). PubMed PMID: [22820288](#); PubMed Central PMCID:
- 586 [PMCPMC3408748](#).
- 587 8. Tsai WC, Hsu SD, Hsu CS, Lai TC, Chen SJ, Shen R, et al. MicroRNA-122 plays a critical
- 588 role in liver homeostasis and hepatocarcinogenesis. *J Clin Invest*. 2012;122(8):2884-97. doi:
- 589 [10.1172/JCI63455](#). PubMed PMID: [22820290](#); PubMed Central PMCID: [PMCPMC3408747](#).
- 590 9. Shimakami T, Yamane D, Jangra RK, Kempf BJ, Spaniel C, Barton DJ, et al. Stabilization
- 591 of hepatitis C virus RNA by an Ago2-miR-122 complex. *Proc Natl Acad Sci U S A*. 2012;109(3):941-6.
- 592 doi: [10.1073/pnas.1112263109](#). PubMed PMID: [22215596](#); PubMed Central PMCID:
- 593 [PMCPMC3271899](#).

- 594 10. Henke JI, Goergen D, Zheng J, Song Y, Schüttler CG, Fehr C, et al. microRNA-122  
595 stimulates translation of hepatitis C virus RNA. *EMBO J.* 2008;27(24):3300-10. doi:  
596 10.1038/emboj.2008.244. PubMed PMID: 19020517; PubMed Central PMCID: PMCPMC2586803.
- 597 11. Roberts AP, Lewis AP, Jopling CL. miR-122 activates hepatitis C virus translation by a  
598 specialized mechanism requiring particular RNA components. *Nucleic Acids Res.*  
599 2011;39(17):7716-29. doi: 10.1093/nar/gkr426. PubMed PMID: 21653556; PubMed Central PMCID:  
600 PMCPMC3177192.
- 601 12. Masaki T, Arend KC, Li Y, Yamane D, McGivern DR, Kato T, et al. miR-122 Stimulates  
602 Hepatitis C Virus RNA Synthesis by Altering the Balance of Viral RNAs Engaged in Replication  
603 versus Translation. *Cell Host Microbe.* 2015;17(2):217-28. doi: 10.1016/j.chom.2014.12.014. PubMed  
604 PMID: 25662750; PubMed Central PMCID: PMCPMC4326553.
- 605 13. Jopling CL, Schütz S, Sarnow P. Position-dependent function for a tandem microRNA  
606 miR-122-binding site located in the hepatitis C virus RNA genome. *Cell Host Microbe.*  
607 2008;4(1):77-85. doi: 10.1016/j.chom.2008.05.013. PubMed PMID: 18621012; PubMed Central  
608 PMCID: PMCPMC3519368.
- 609 14. Machlin ES, Sarnow P, Sagan SM. Masking the 5' terminal nucleotides of the hepatitis C  
610 virus genome by an unconventional microRNA-target RNA complex. *Proc Natl Acad Sci U S A.*  
611 2011;108(8):3193-8. doi: 10.1073/pnas.1012464108. PubMed PMID: 21220300; PubMed Central  
612 PMCID: PMCPMC3044371.
- 613 15. Jopling CL. Regulation of hepatitis C virus by microRNA-122. *Biochem Soc Trans.*  
614 2008;36(Pt 6):1220-3. doi: 10.1042/BST0361220. PubMed PMID: 19021529.
- 615 16. Li Y, Masaki T, Yamane D, McGivern DR, Lemon SM. Competing and noncompeting  
616 activities of miR-122 and the 5' exonuclease Xrn1 in regulation of hepatitis C virus replication. *Proc*  
617 *Natl Acad Sci U S A.* 2013;110(5):1881-6. doi: 10.1073/pnas.1213515110. PubMed PMID: 23248316;  
618 PubMed Central PMCID: PMCPMC3562843.
- 619 17. Sedano CD, Sarnow P. Hepatitis C virus subverts liver-specific miR-122 to protect the viral  
620 genome from exoribonuclease Xrn2. *Cell Host Microbe.* 2014;16(2):257-64. doi:  
621 10.1016/j.chom.2014.07.006. PubMed PMID: 25121753; PubMed Central PMCID:  
622 PMCPMC4227615.

- 623 18. Li Y, Yamane D, Lemon SM. Dissecting the roles of the 5' exoribonucleases Xrn1 and Xrn2  
624 in restricting hepatitis C virus replication. *J Virol.* 2015;89(9):4857-65. doi: 10.1128/JVI.03692-14.  
625 PubMed PMID: 25673723; PubMed Central PMCID: PMC4403451.
- 626 19. Luna JM, Scheel TK, Danino T, Shaw KS, Mele A, Fak JJ, et al. Hepatitis C Virus RNA  
627 Functionally Sequesters miR-122. *Cell.* 2015;160(6):1099-110. doi: 10.1016/j.cell.2015.02.025.  
628 PubMed PMID: 25768906.
- 629 20. Schult P, Roth H, Adams RL, Mas C, Imbert L, Orlik C, et al. microRNA-122 amplifies  
630 hepatitis C virus translation by shaping the structure of the internal ribosomal entry site. *Nat Commun.*  
631 2018;9(1):2613. Epub 2018/07/06. doi: 10.1038/s41467-018-05053-3. PubMed PMID: 29973597;  
632 PubMed Central PMCID: PMC6031695.
- 633 21. Amador-Canizares Y, Panigrahi M, Huys A, Kunden RD, Adams HM, Schinold MJ, et al.  
634 miR-122, small RNA annealing and sequence mutations alter the predicted structure of the Hepatitis C  
635 virus 5' UTR RNA to stabilize and promote viral RNA accumulation. *Nucleic Acids Res.* 2018. Epub  
636 2018/07/28. doi: 10.1093/nar/gky662. PubMed PMID: 30053137.
- 637 22. Yokoyama T, Machida K, Iwasaki W, Shigeta T, Nishimoto M, Takahashi M, et al. HCV  
638 IRES Captures an Actively Translating 80S Ribosome. *Mol Cell.* 2019;74(6):1205-14.e8. Epub  
639 2019/05/09. doi: 10.1016/j.molcel.2019.04.022. PubMed PMID: 31080011.
- 640 23. Ono C, Fukuhara T, Motooka D, Nakamura S, Okuzaki D, Yamamoto S, et al.  
641 Characterization of miR-122-independent propagation of HCV. *PLoS Pathog.* 2017;13(5):e1006374.  
642 Epub 2017/05/12. doi: 10.1371/journal.ppat.1006374. PubMed PMID: 28494029; PubMed Central  
643 PMCID: PMC5441651.
- 644 24. Israelow B, Mullokandov G, Agudo J, Sourisseau M, Bashir A, Maldonado AY, et al.  
645 Hepatitis C virus genetics affects miR-122 requirements and response to miR-122 inhibitors. *Nat*  
646 *Commun.* 2014;5:5408. doi: 10.1038/ncomms6408. PubMed PMID: 25403145; PubMed Central  
647 PMCID: PMC4236719.
- 648 25. Cong L, Ran FA, Cox D, Lin S, Barretto R, Habib N, et al. Multiplex genome engineering  
649 using CRISPR/Cas systems. *Science.* 2013;339(6121):819-23. doi: 10.1126/science.1231143. PubMed  
650 PMID: 23287718; PubMed Central PMCID: PMC3795411.

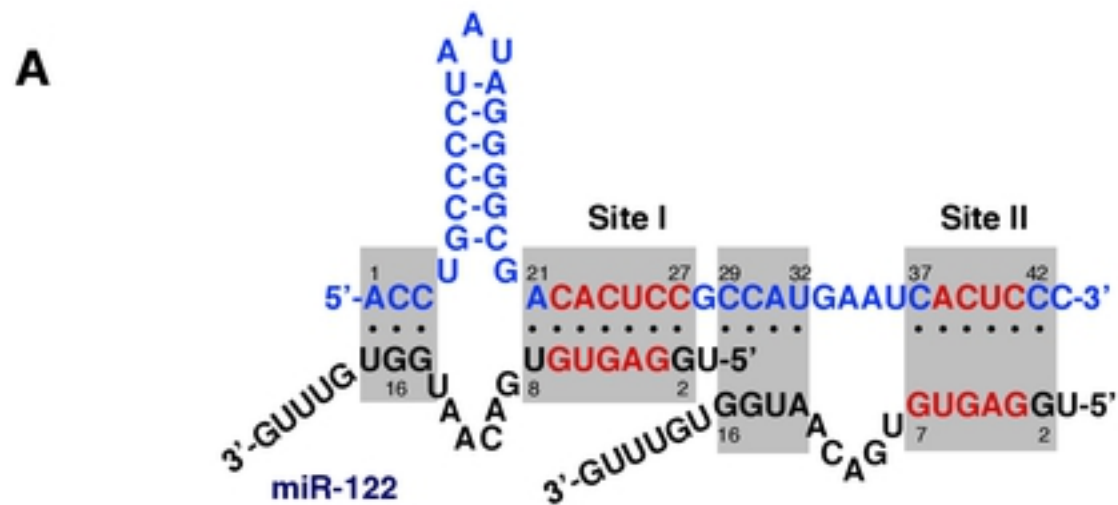
- 651 26. Mali P, Yang L, Esvelt KM, Aach J, Guell M, DiCarlo JE, et al. RNA-guided human  
652 genome engineering via Cas9. *Science*. 2013;339(6121):823-6. doi: 10.1126/science.1232033. PubMed  
653 PMID: 23287722; PubMed Central PMCID: PMC3712628.
- 654 27. Wakita T, Pietschmann T, Kato T, Date T, Miyamoto M, Zhao Z, et al. Production of  
655 infectious hepatitis C virus in tissue culture from a cloned viral genome. *Nat Med*. 2005;11(7):791-6.  
656 doi: 10.1038/nm1268. PubMed PMID: 15951748; PubMed Central PMCID: PMC2918402.
- 657 28. Das MK, Andreassen R, Haugen TB, Furu K. Identification of Endogenous Controls for Use  
658 in miRNA Quantification in Human Cancer Cell Lines. *Cancer Genomics Proteomics*. 2016;13(1):63-8.  
659 Epub 2015/12/29. PubMed PMID: 26708600.
- 660 29. Sharma S, Ding F, Dokholyan NV. iFoldRNA: three-dimensional RNA structure prediction  
661 and folding. *Bioinformatics*. 2008;24(17):1951-2. Epub 2008/06/25. doi:  
662 10.1093/bioinformatics/btn328. PubMed PMID: 18579566; PubMed Central PMCID:  
663 PMC2559968.
- 664 30. Krokhotin A, Houlihan K, Dokholyan NV. iFoldRNA v2: folding RNA with constraints.  
665 *Bioinformatics*. 2015;31(17):2891-3. Epub 2015/04/24. doi: 10.1093/bioinformatics/btv221. PubMed  
666 PMID: 25910700; PubMed Central PMCID: PMC4547609.
- 667 31. Ding F, Tsao D, Nie H, Dokholyan NV. Ab initio folding of proteins with all-atom discrete  
668 molecular dynamics. *Structure*. 2008;16(7):1010-8. doi: 10.1016/j.str.2008.03.013. PubMed PMID:  
669 18611374; PubMed Central PMCID: PMC2533517.
- 670 32. Proctor E, Ding F, Dokholyan N. Discrete molecular dynamics. *Wiley Interdisciplinary*  
671 *Reviews-Computational Molecular Science*. 2011;1(1):80-92. doi: 10.1002/wcms.4. PubMed PMID:  
672 WOS:000295991000008.
- 673 33. Zhang W, Thevapriya S, Kim PJ, Yu WP, Je HS, Tan EK, et al. Amyloid precursor protein  
674 regulates neurogenesis by antagonizing miR-574-5p in the developing cerebral cortex. *Nat Commun*.  
675 2014;5:3330. Epub 2014/03/04. doi: 10.1038/ncomms4330. PubMed PMID: 24584353.
- 676 34. Ludwig N, Leidinger P, Becker K, Backes C, Fehlmann T, Pallasch C, et al. Distribution of  
677 miRNA expression across human tissues. *Nucleic Acids Res*. 2016;44(8):3865-77. Epub 2016/02/28.  
678 doi: 10.1093/nar/gkw116. PubMed PMID: 26921406; PubMed Central PMCID: PMC4856985.



- 679 35. Chahal J, Gebert LFR, Gan HH, Camacho E, Gunsalus KC, MacRae IJ, et al. miR-122 and  
680 Ago interactions with the HCV genome alter the structure of the viral 5' terminus. *Nucleic Acids Res.*  
681 2019;47(10):5307-24. doi: 10.1093/nar/gkz194. PubMed PMID: 30941417; PubMed Central PMCID:  
682 PMC6547439.
- 683 36. Bogerd HP, Kennedy EM, Whisnant AW, Cullen BR. Induced Packaging of Cellular  
684 MicroRNAs into HIV-1 Virions Can Inhibit Infectivity. *MBio.* 2017;8(1). Epub 2017/01/18. doi:  
685 10.1128/mBio.02125-16. PubMed PMID: 28096489; PubMed Central PMCID: PMC5241401.
- 686 37. Huang J, Wang F, Argyris E, Chen K, Liang Z, Tian H, et al. Cellular microRNAs  
687 contribute to HIV-1 latency in resting primary CD4+ T lymphocytes. *Nat Med.* 2007;13(10):1241-7.  
688 Epub 2007/10/02. doi: 10.1038/nm1639. PubMed PMID: 17906637.
- 689 38. Shi G, Ando T, Suzuki R, Matsuda M, Nakashima K, Ito M, et al. Involvement of the 3'  
690 Untranslated Region in Encapsidation of the Hepatitis C Virus. *PLoS Pathog.* 2016;12(2):e1005441.  
691 Epub 2016/02/13. doi: 10.1371/journal.ppat.1005441. PubMed PMID: 26867128; PubMed Central  
692 PMCID: PMC4750987.
- 693 39. Friebe P, Bartenschlager R. Role of RNA structures in genome terminal sequences of the  
694 hepatitis C virus for replication and assembly. *J Virol.* 2009;83(22):11989-95. Epub 2009/09/11. doi:  
695 10.1128/jvi.01508-09. PubMed PMID: 19740989; PubMed Central PMCID: PMC2772684.
- 696 40. Preciado MV, Valva P, Escobar-Gutierrez A, Rahal P, Ruiz-Tovar K, Yamasaki L, et al.  
697 Hepatitis C virus molecular evolution: transmission, disease progression and antiviral therapy. *World J*  
698 *Gastroenterol.* 2014;20(43):15992-6013. doi: 10.3748/wjg.v20.i43.15992. PubMed PMID: 25473152;  
699 PubMed Central PMCID: PMC4239486.
- 700 41. Lavanchy D. Evolving epidemiology of hepatitis C virus. *Clin Microbiol Infect.*  
701 2011;17(2):107-15. doi: 10.1111/j.1469-0691.2010.03432.x. PubMed PMID: 21091831.
- 702 42. Zhou R, Zhou X, Yin Z, Guo J, Hu T, Jiang S, et al. MicroRNA-574-5p promotes metastasis  
703 of non-small cell lung cancer by targeting PTPRU. *Sci Rep.* 2016;6:35714. Epub 2016/10/21. doi:  
704 10.1038/srep35714. PubMed PMID: 27761023; PubMed Central PMCID: PMC5071770.
- 705 43. Zhou R, Zhou X, Yin Z, Guo J, Hu T, Jiang S, et al. Tumor invasion and metastasis  
706 regulated by microRNA-184 and microRNA-574-5p in small-cell lung cancer. *Oncotarget.*

- 707 2015;6(42):44609-22. Epub 2015/11/21. doi: 10.18632/oncotarget.6338. PubMed PMID: 26587830;  
708 PubMed Central PMCID: PMC4792579.
- 709 44. Li Q, Li X, Guo Z, Xu F, Xia J, Liu Z, et al. MicroRNA-574-5p was pivotal for TLR9  
710 signaling enhanced tumor progression via down-regulating checkpoint suppressor 1 in human lung  
711 cancer. PLoS One. 2012;7(11):e48278. Epub 2012/11/08. doi: 10.1371/journal.pone.0048278. PubMed  
712 PMID: 23133627; PubMed Central PMCID: PMC3487732.
- 713 45. Zhang S, Zhang Y, Cheng Q, Ma Z, Gong G, Deng Z, et al. Silencing protein kinase C zeta  
714 by microRNA-25-5p activates AMPK signaling and inhibits colorectal cancer cell proliferation.  
715 Oncotarget. 2017;8(39):65329-38. Epub 2017/10/17. doi: 10.18632/oncotarget.18649. PubMed PMID:  
716 29029434; PubMed Central PMCID: PMC5630334.
- 717 46. Zhang BB, Zhou G, Li C. AMPK: an emerging drug target for diabetes and the metabolic  
718 syndrome. Cell Metab. 2009;9(5):407-16. Epub 2009/05/07. doi: 10.1016/j.cmet.2009.03.012. PubMed  
719 PMID: 19416711.

720



bioRxiv preprint doi: <https://doi.org/10.1101/2020.01.10.901488>; this version posted January 10, 2020. The copyright holder for this preprint (which was not certified by peer review) is the author/funder, who has granted bioRxiv a license to display the preprint in perpetuity. It is made available under aCC-BY 4.0 International license.

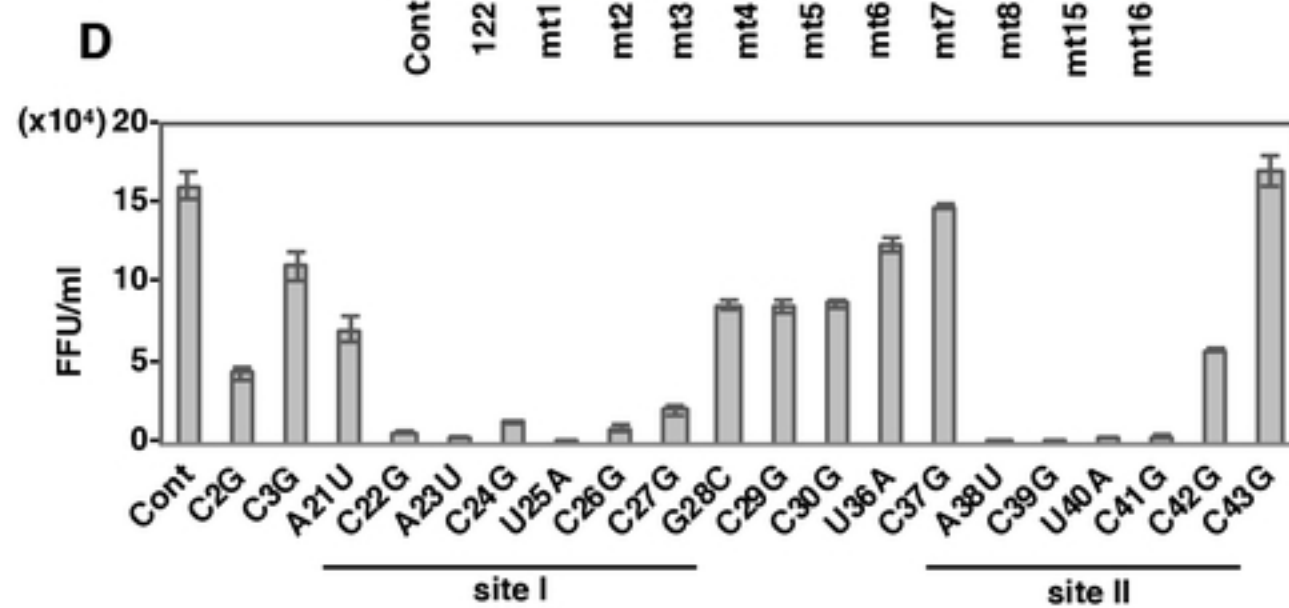
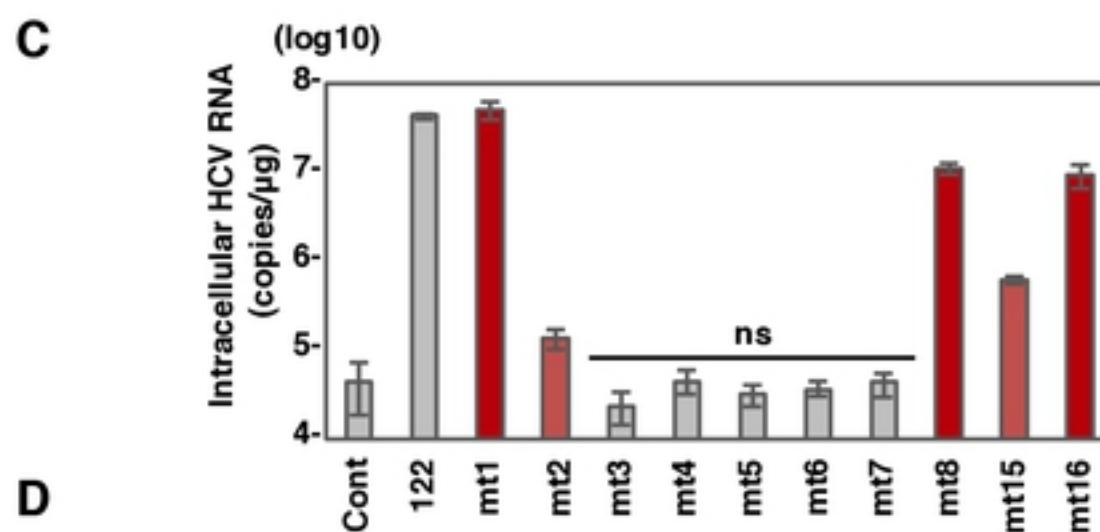
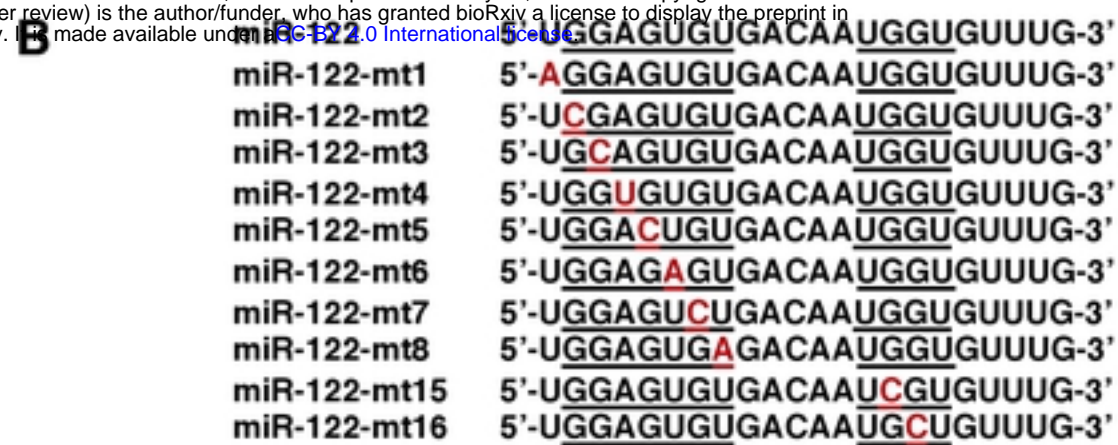
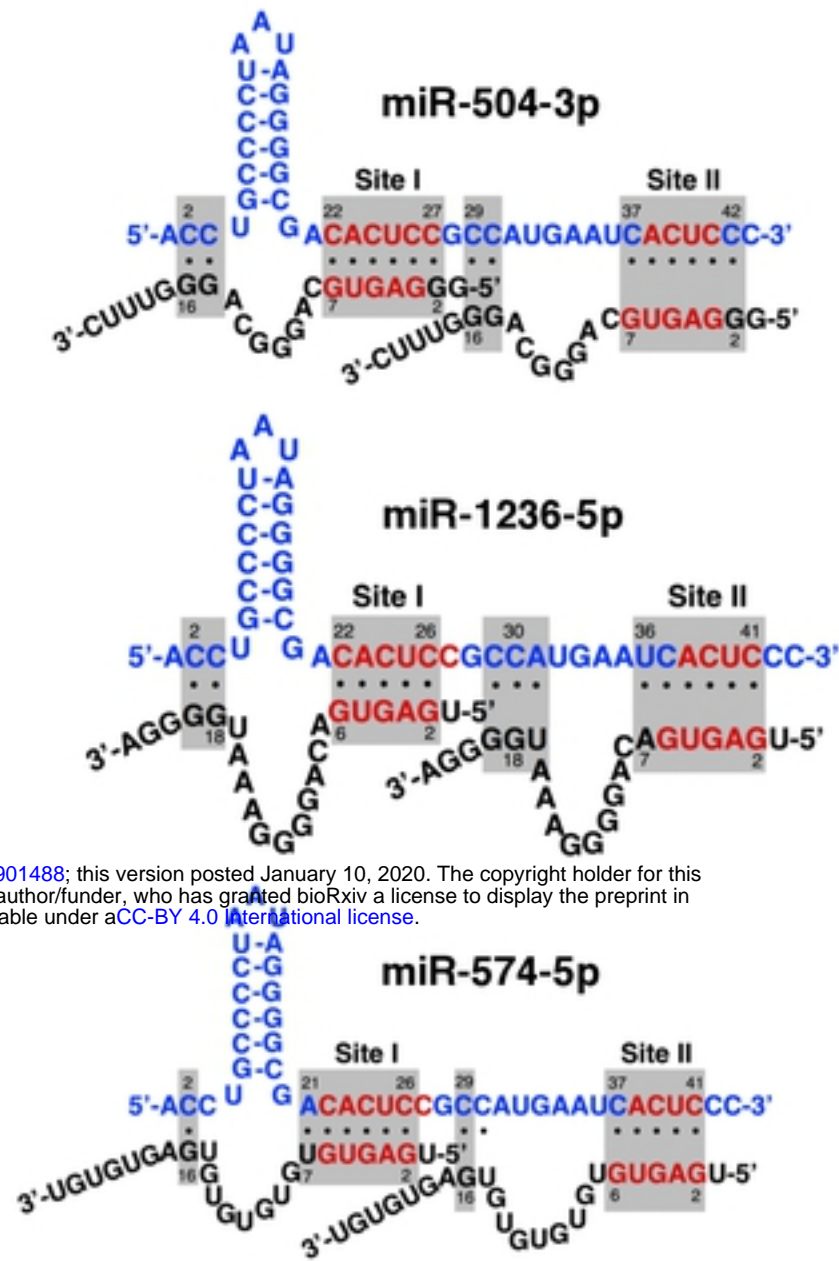


Figure 1

**A**



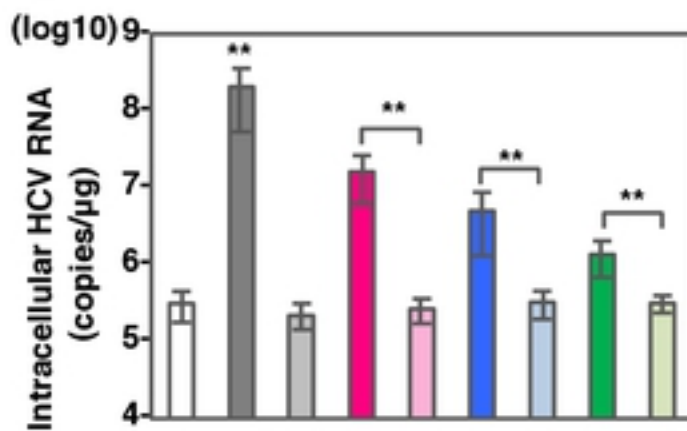
bioRxiv preprint doi: <https://doi.org/10.1101/2020.01.10.901488>; this version posted January 10, 2020. The copyright holder for this preprint (which was not certified by peer review) is the author/funder, who has granted bioRxiv a license to display the preprint in perpetuity. It is made available under aCC-BY 4.0 International license.

**B**

**GAGUG motif**

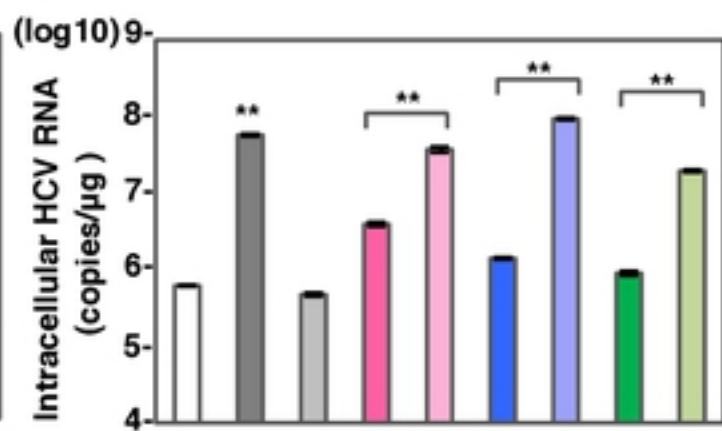
miR-122	5'-UGGAGUGUGACAAUGGUGUUUG-3'
<b>miR-504-3p</b>	5'-GGGAGUG <b>C</b> AGGGCAGGGUUUC-3'
miR-504-3p-mt6	5'-GGGAGU <b>A</b> CAGGGCAGGGUUUC-3'
miR-504-3p-mt8	5'-GGGAGUG <b>U</b> AGGGCAGGGUUUC-3'
<b>miR-574-5p</b>	5'- <b>U</b> GAGUGUGUGUGUGUGAGUGUGU-3'
miR-574-5p-mt5	5'- <b>U</b> GAG <b>A</b> GUGUGUGUGUGAGUGUGU-3'
miR-574-5p-addG	5'- <b>U</b> GGAGUGUGUGUGUGUGAGUGUGU-3'
<b>miR-1236-5p</b>	5'- <b>U</b> GAGUGACAGGGGAAAUGGGGA-3'
miR-1236-5p-mt5	5'- <b>U</b> GAG <b>A</b> GACAGGGGAAAUGGGGA-3'
miR-1236-5p-addG	5'- <b>U</b> GGAGUGACAGGGGAAAUGGGGA-3'

**C**



□ control  
 ■ miR-122    ■ miR-122-mt6  
 ■ miR-504-3p    ■ miR-504-3p-mt6  
 ■ miR-574-5p    ■ miR-574-5p-mt5  
 ■ miR-1236-5p    ■ miR-1236-5p-mt5

**D**



□ control  
 ■ miR-122    ■ miR-122-mt6  
 ■ miR-504-3p    ■ miR-504-3p-mt8  
 ■ miR-574-5p    ■ miR-574-5p-addG  
 ■ miR-1236-5p    ■ miR-1236-5p-addG

bioRxiv preprint doi: <https://doi.org/10.1101/2020.01.10.991488>; this version posted January 10, 2020. The copyright holder for this preprint (which was not certified by peer review) is the author/funder, who has granted bioRxiv a license to display the preprint in perpetuity. It is made available under aCC-BY 4.0 International license.

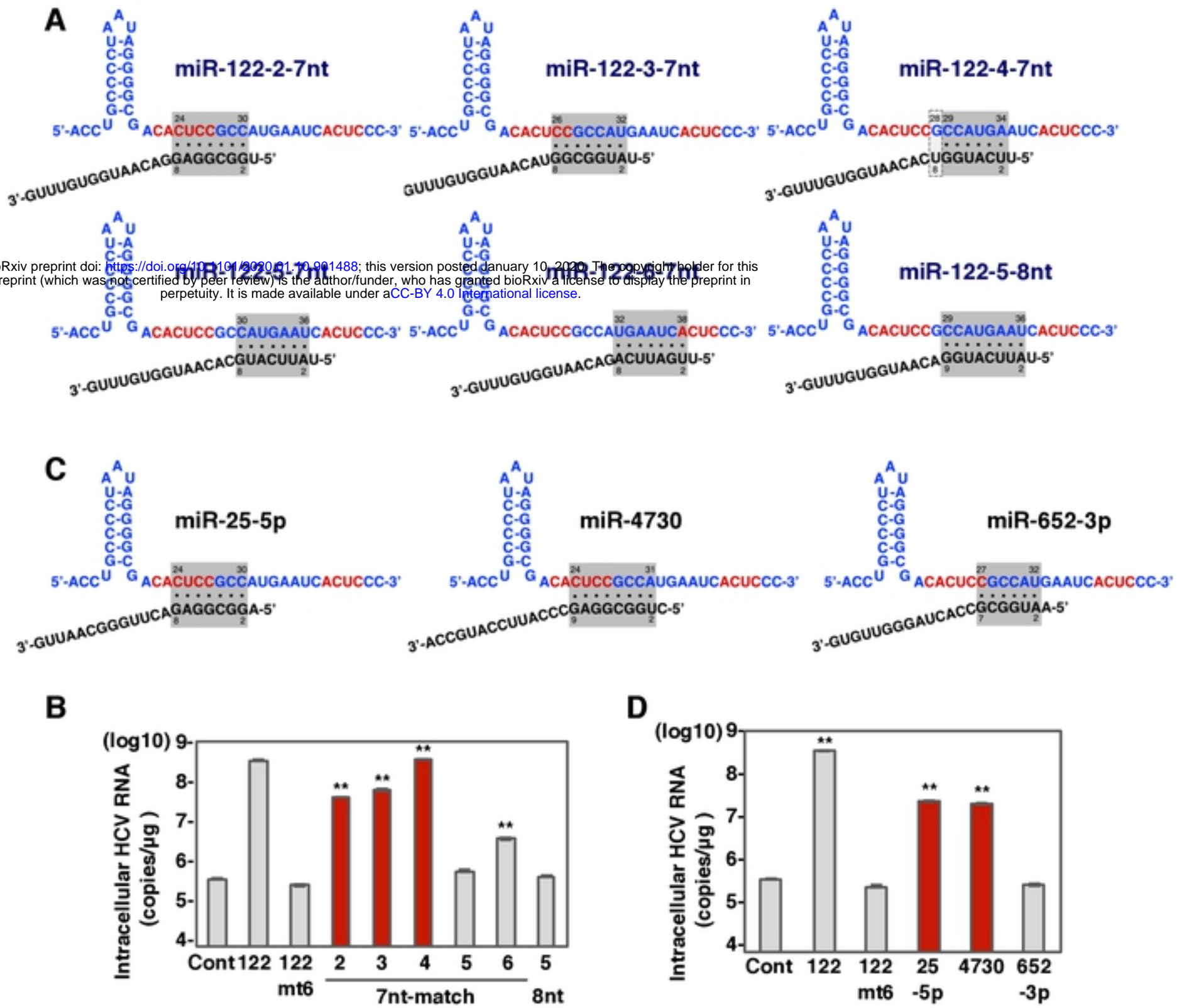


Figure3

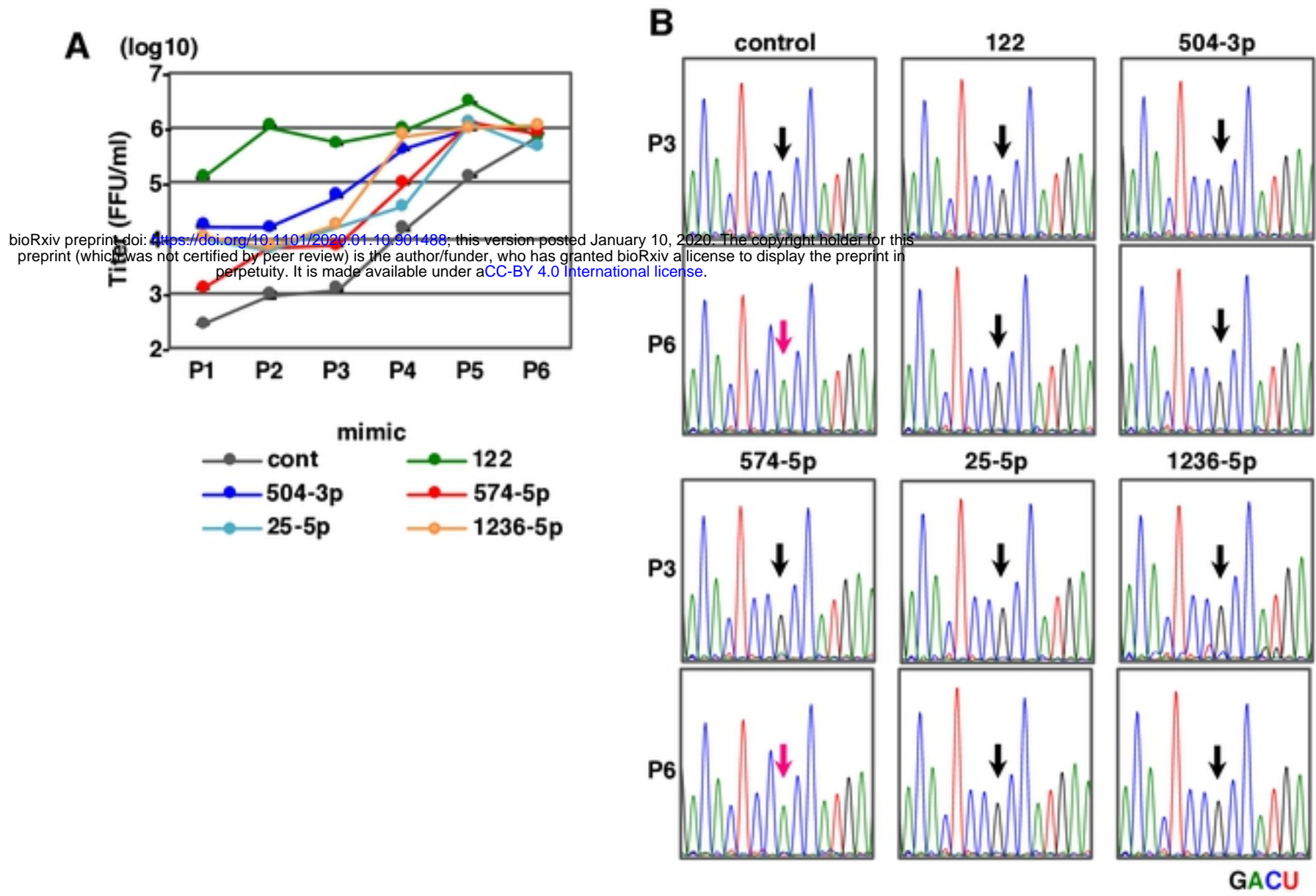


Figure4

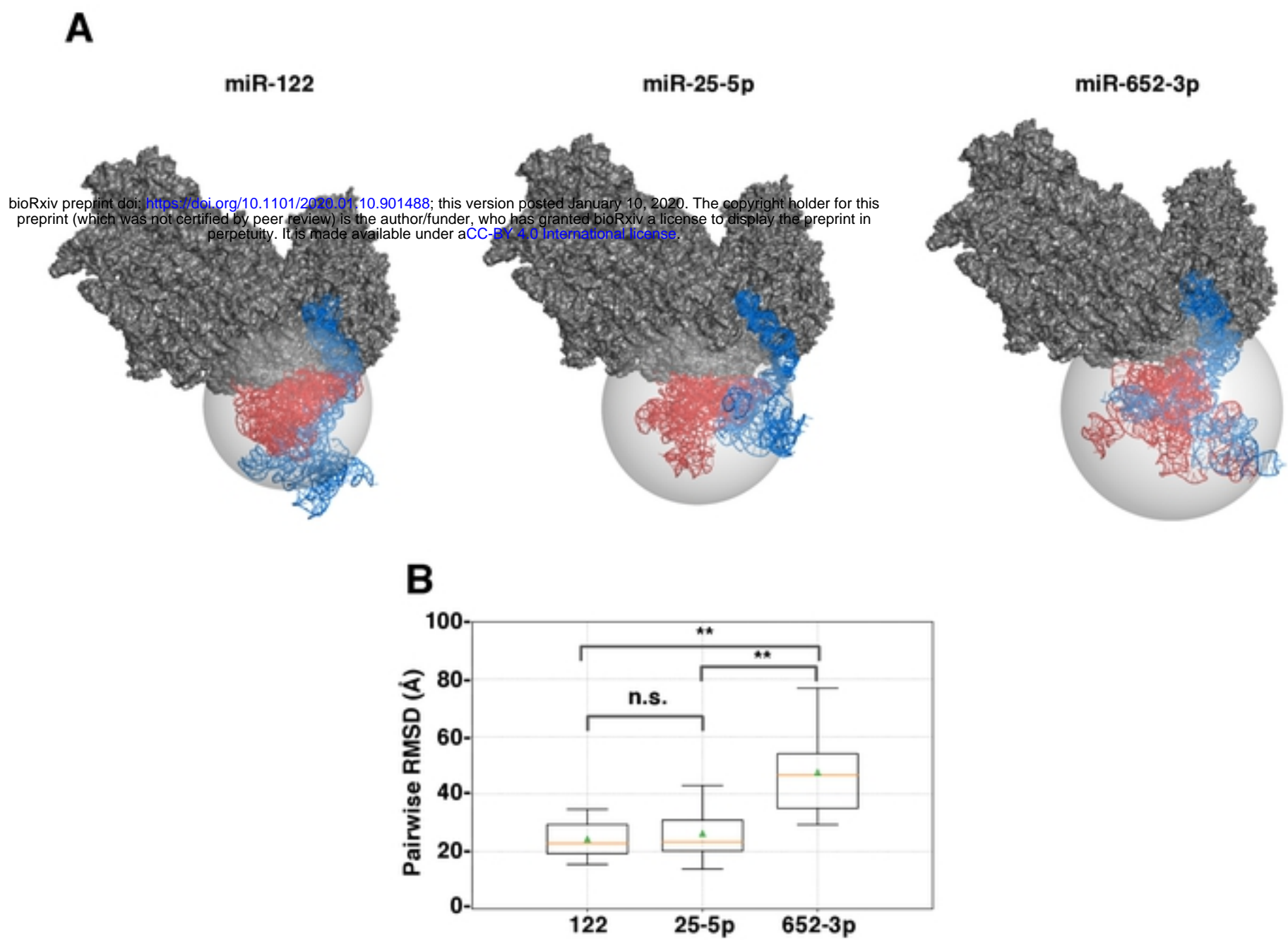


Figure5